ACS PHYSICAL CHEMISTRY Au
AN OPEN ACCESS JOURNAL OF THE AMERICAN CHEMICAL SOCIETY

pubs.acs.org/physchemau

Article

Exploring Solvent Effects on the Proton Transfer Processes of Selected Benzoxazole Derivatives by Femtosecond Time-Resolved Fluorescence and Transient Absorption Spectroscopies

Runhui Liang, Yuanchun Li, Zhiping Yan, Xueqin Bai, Wenquan Lai, Lili Du,* and David Lee Phillips*

Cite This: *ACS Phys. Chem Au* 2023, 3, 181−189

Read Online

ACCESS | Metrics & More | Article Recommendations | Supporting Information

ABSTRACT: Excited-state intramolecular proton transfer (ESIPT) is of great importance due to the large Stokes shift emission that can be observed in some ESIPT molecules. Although steady-state spectroscopies have been employed to study the properties of some ESIPT molecules, their excited-state dynamics have not been examined directly with time-resolved spectroscopy methods yet for a number of systems. Here, an in-depth investigation of the solvent effects on the excited-state dynamics of two prototypical ESIPT molecules, 2-(2′-hydroxyphenyl)-benzoxazole (**HBO**) and 2-(2′-hydroxynaphthalenyl)-benzoxazole (**NAP**), have been accomplished by using femtosecond time-resolved fluorescence and transient absorption spectroscopies. Solvent effects affect the excited-state dynamics of **HBO** more significantly than that of **NAP**. Particularly in the presence of water, the photodynamics pathways of **HBO** are changed, while only small changes can be found in **NAP**. An ultrafast ESIPT process that occurs within our instrumental response is observed for **HBO**, and this is followed by an isomerization process in ACN solution. However, in aqueous solution, the obtained *syn*-keto* after ESIPT can be solvated by water in about 3.0 ps, and the isomerization process is totally inhibited for **HBO**. The mechanism of **NAP** is different from **HBO** and is determined to be a two-step excited-state proton transfer process. Upon photoexcitation, **NAP** is deprotonated first in the excited state to generate the anion*, which can transfer to the *syn*-keto* form followed by an isomerization process.

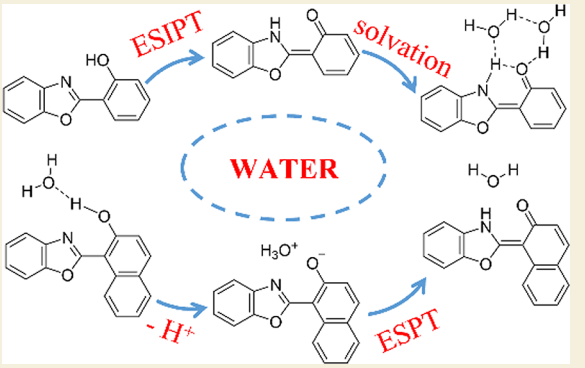

KEYWORDS: *ultrafast spectroscopy, excited-state dynamics, ESIPT, ESPT, deprotonation*

INTRODUCTION

Since the first report by Weller,[1] excited-state intramolecular proton transfer (ESIPT) has received great research interest and has been applied in various fields due to the abnormally large Stokes shift between the fluorescence and absorption spectra observed for a variety of molecules.[2−6] Many fluorophores have demonstrated ESIPT character, such as the derivatives of benzoxazole,[7−10] benzophenones,[11] flavones,[12] anthraquinones,[13,14] quinolines,[15] and so on. Recently, selective ESIPT fluorophores were used as building blocks to construct novel covalent−organic frameworks and aggregation-induced emission functional materials.[16−18] To rationalize the design criteria on ESIPT molecules and ESIPT-based functional materials, it is crucial to understand the factors that affect the photophysical mechanisms of ESIPT processes and their subsequent reactions in depth.

Generally, ESIPT is an intriguing photoinduced singlet-excited-state enol (enol*) to singlet-excited-state keto (keto*) tautomerization reaction in a four-level photocycle containing the tautomers in their ground states and excited states (Scheme S1).[19] The prerequisite for ESIPT molecules is the intramolecular hydrogen bonding interaction between a proton-donating group (such as hydroxyl or amino groups) and a neighboring proton-accepting group (such as a carbonyl group or a nitrogen atom in a heterocycle) within 2 Å. The ESIPT molecules are easily characterized with the steady-state absorption and emission spectroscopies: similar absorbance to the parent compounds while a large Stokes shift emission may be observed in the ESIPT molecules.[20] Typically, most ESIPT molecules show dual emission bands with an enol* emission band located at a shorter wavelength and a keto* emission band demonstrating an enhanced Stokes shift (~200 nm), which can avoid the inner filter effect or self-reabsorption effects and makes ESIPT molecules promising candidates for fluorophores. Many ESIPT molecules have been reported, such as 2-(2′-hydroxyphenyl)-benzoxazole (**HBO**),[9,21] 2-(2′-hy-

Received: August 8, 2022
Revised: December 14, 2022
Accepted: December 15, 2022
Published: December 23, 2022

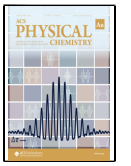

Scheme 1. (a) Chemical Structures of HBO and NAP; (b) Isomers and Tautomer of HBO

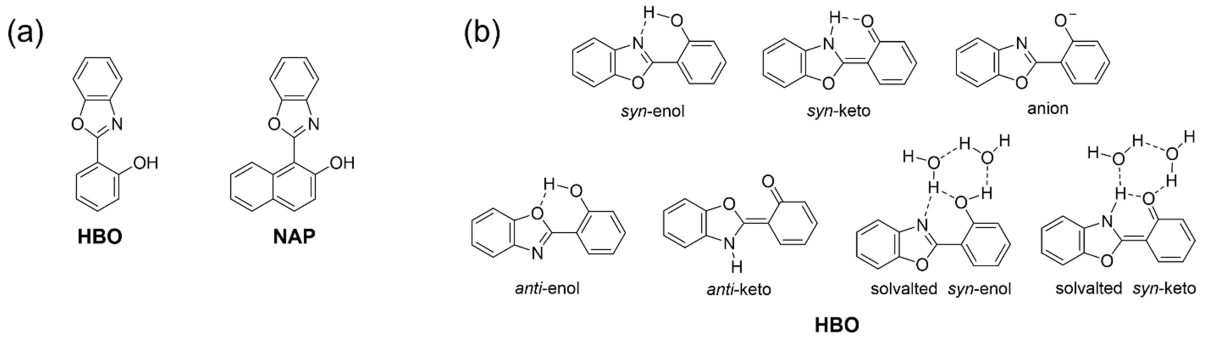

droxyphenyl)-benzothiazole,[18,22,23] 2-(2′-hydroxynaphthalenyl)-benzoxazole (**NAP**),[8] and 3-hydroxyflavone.[24−26] Two of the most popular benzoxazole-based ESIPT chromophores, **HBO** and its naphthyl-fused analog **NAP** (the structures are shown in Scheme 1a), were chosen as the model compounds to be discussed in this article because of their interesting emission behavior and simple structural modification.

In general, both absorption and emission bands redshift when the aromatic ring expands from benzene to naphthalene. Indeed, **NAP** showed a redshifted absorption maximum that is around 40 nm longer than that of **HBO**, while the keto* emission of **NAP** appeared at a shorter wavelength (460 nm) with a lower quantum yield (0.003) than that of **HBO** (λ = 508 nm, Φ_f = 0.02) in toluene.[8,10] The origin of this unconventional emission phenomenon was explained by VanVeller and coworkers using Baird's rule, suggesting that the greater aromaticity in the ground state results in the greater antiaromaticity in the singlet excited state and *vice versa*.[7] The less antiaromatic enol* for **NAP** had a smaller driving force to produce the keto* tautomer and resulted in a larger energy gap between keto* and keto in **NAP** relative to that of **HBO**. Although the ESIPT tautomers of **HBO** and **NAP** have been characterized using steady-state fluorescence spectroscopy, the photophysical and photochemical dynamics of the molecules are still obscure. For instance, what is the ultrafast ESIPT rate and what are the subsequent reactions of *syn*-keto*? Therefore, time-resolved spectroscopies and quantum chemical calculations were employed to address these issues.[10,27−31] It was reported that ESIPT took place in the *syn*-enol* molecules with an intramolecular O−H−N hydrogen bond only.[32] Upon photoexcitation, the most stable *syn*-enol form of **HBO** and **NAP** was photoexcited to *syn*-enol*, which was transformed to *syn*-keto* through an ESIPT process. With the help of time-resolved spectroscopies, the rapid ESIPT lifetime of **HBO** was determined to be around 150[31] and 80−90 fs,[21] while little was known about **NAP** in this regard. Moreover, as determined by time-resolved fluorescence spectroscopy (TRF), the lifetimes of *syn*-keto* and *anti*-enol* in **HBO** were 295 and 1370 ps in hexane, respectively.[27] Based on the reported results, the ESIPT can be observed in different solvents in **HBO**, while the fluorescence lifetime of the *syn*-keto* decreases dramatically in the polar solvents.[27] Also, the fluorescence lifetime of the *syn*-keto* is much shorter for **NAP** than that of **HBO**.[10] In addition, another two transient species are observed in the nanosecond time-resolved transient absorption spectroscopy (ns-TA) measurements, and they cannot be attributed to the absorption of the *syn*-keto* and *anti*-enol* intermediates due to the big differences in their lifetimes. Furthermore, these species are finally confirmed by results from quenching experiments, in which one species corresponded to the triplet excited state of *syn*-keto* (an oxygen sensitive species) via intersystem crossing (ISC) and another is attributed to the ground-state *anti*-keto (a proton-sensitive species) via an isomerization process, and these dynamics are similar to the observations for **NAP** as well.[10,30] Simple photodynamics decay pathways of the *syn*-enol form of **HBO** and **NAP** are displayed in Scheme S2, and the time constants measured by TRF and ns-TA are also summarized in Table S1.

It seems that the photochemical and photophysical mechanisms of **HBO** and **NAP** have been mostly explained, but there are still some remaining questions that need to be addressed. For example, a new species with a new emission band is observed for **HBO** in the aqueous solutions,[33] while little efforts have been achieved to study this new species and its relation between the ESIPT process. Femtosecond time-resolved fluorescence spectroscopy (fs-TRF) and time-resolved transient absorption spectroscopy (fs-TA) experiments with the demonstration of spectral changes and the kinetics study can be very useful in helping to further elucidate the photophysical mechanisms of **HBO** and **NAP**. The fs-TRF and fs-TA measurements were performed on **HBO** and **NAP** in different solvents and particularly in aqueous environments to better understand how the varying solvent properties influence the photophysical mechanisms in these molecules. Water played an important role in the ESIPT process of **HBO**, while little difference was obtained in pure acetonitrile (ACN) and aqueous solution for **NAP**, which indicates that **NAP** may adapt the excited-state proton transfer (ESPT) reaction instead. This study provides critical insights into the solvent effects on the ultrafast dynamics of **HBO** and **NAP**, which can potentially benefit the design of related ESIPT molecules and functional materials with ESIPT character.

MATERIALS AND METHODS

Materials

HBO was purchased from TCI Company and used as received.

Synthesis of NAP

NAP was synthesized according to the synthetic route as shown in Scheme S3.[8] Specifically, into a 25 mL round-bottom flask, 2-aminophenol (109 mg, 1 mmol) and 2-hydroxy-1-naphthaldehyde (172 mg, 1 mmol) were dissolved in 10 mL of ethanol with a catalytic amount of acetic acid. After the mixture was refluxed for 4 h, the solution was allowed to cool down to room temperature. The precipitate formed was filtered, washed with cold ethanol, and dried under vacuum to get the product, which was used in the following reaction without further purification. The product from the last step (210 mg, 0.80 mmol) and 2,3-dichloro-5,6-dicyano-1,4-benzoquinone (DDQ, 204 mg, 0.9 mmol) were added into 80 mL of anhydrous

https://doi.org/10.1021/acsphyschemau.2c00036
ACS Phys. Chem Au 2023, 3, 181−189

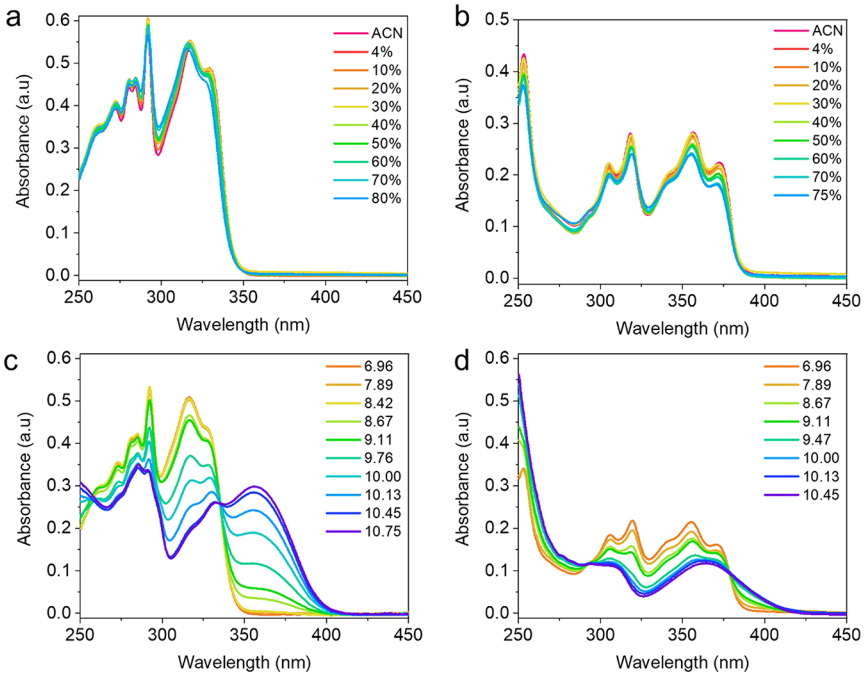

Figure 1. Absorption spectra of **HBO** (a) and **NAP** (b) in different fractions of H_2O into ACN solutions. The absorption spectra of **HBO** (c) and **NAP** (d) with increasing pH values in ACN:buffer (1,4) mixed solutions. The concentrations of **HBO** and **NAP** are around 10^{-5} mol/L.

chloroform, and the mixture was reacted at room temperature. After an overnight reaction, the solution was washed with saturated $NaHCO_3$ solution three times, and the organic phase was collected and evaporated. The residue was purified by silica gel column chromatography (hexane:ethyl acetate = 4:1) to give the final product **NAP** in a solid form (46 mg, 0.18 mmol) in 22% yield. ^{1}H NMR (500 MHz, $CDCl_3$): δ 13.51 (s, 1H), 9.12 (d, J = 8.7 Hz, 1H), 7.91 (d, J = 8.9 Hz, 1H), 7.83 (d, J = 8.1 Hz, 1H), 7.81−7.76 (m, 1H), 7.76−7.71 (m, 1H), 7.67 (t, J = 7.8 Hz, 1H), 7.43 (td, J = 6.3, 3.2 Hz, 3H), 7.34 (d, J = 8.9 Hz, 1H); ^{13}C{^{1}H} NMR (126 MHz, $CDCl_3$): δ 164.96, 161.20, 149.07, 138.60, 134.98, 131.07, 129.31, 128.70, 128.56, 125.38, 125.32, 124.69, 123.91, 119.57, 118.91, 110.89, 102.59; HRMS (ESI-QTOF): m/z [M + H]$^+$ calcd. for $C_{17}H_{12}N_1O_2$, 262.0868; found, 262.0862.

Setup of fs-TA

A general description on this setup and methods are given here, while details can be found in our previous study.[34] Amplified laser pulses (800 nm) were seeded from a femtosecond regenerative amplified Ti:sapphire laser system and split into a pump laser beam and a probe laser beam for use in the fs-TA experiments. The probe laser pulse was produced by utilizing ∼5% of the amplified 800 nm laser pulses to generate a white-light continuum (325−650 nm) in a CaF_2 crystal, and the pump beam was adjusted at 267 nm. The maximum temporal delay line in this instrument was 3 ns. So, the time constant representing the decay of the last intermediate observed in the fs-TA was given as >3 ns. All sample solutions with an absorbance of 1 at 267 nm were excited in a fixed 2 mm path-length quartz cuvette. The ratios of water and ACN indicated in the article are the volume ratio.

Setup of fs-TRF

The fs-TRF measurement was implemented on the same machine as fs-TA, from which the output 800 nm laser pulse and the third harmonic (267 nm) laser pulse were used as a gate pulse and a pump pulse, respectively. Upon 267 nm excitation, the sample fluorescence was focused into the nonlinear BBO crystal mixing with the gate pulse to generate the sum frequency signal. Broadband fluorescence spectra were obtained by changing the crystal angles, and the spectra were detected by an air-cooled CCD. For the experiment in this work, samples were prepared in a 2 mm path-length cuvette, and the absorbance was 1 at 267 nm.

RESULTS AND DISCUSSION

Steady-State Absorption and Fluorescence Spectra

To identify the deprotonation processes in the ground state and the singlet excited states of **HBO** and **NAP**, steady-state absorption and fluorescence experiments were performed for both **HBO** and **NAP** in aqueous solutions with various fractions of water and also varying pH values. The UV−vis absorption spectra changes of **HBO** and **NAP** with increasing the fractions of H_2O in ACN solutions are shown in Figure 1a,b. In pure ACN solution, **HBO** shows two low-energy $\pi-\pi^*$ transitions at 317 and 330 nm: the former absorption band is assigned to the absorption of *anti*-enol, while the latter is attributed to the absorption of *syn*-enol.[33] **NAP** shows a redshifted absorbance at 356 and 372 nm in pure ACN solution in comparison with **HBO**. Upon increasing the percentage of H_2O in ACN/H_2O mixed solutions, the absorption spectra of both **HBO** and **NAP** show slight blueshifting with a little decrease in intensity, implying that no big changes occur on the molecular geometries and the small blueshifting may be induced by the intermolecular hydrogen-bonding between water and **HBO**/**NAP**.[33] However, progressive differences are found when increasing the pH values of the solutions for both **HBO** and **NAP**. As depicted in Figure 1c, the absorption bands of **HBO** at 317 and 330 nm decrease and give rise to the peak at 375 nm with an isosbestic point at 335 nm upon changing from neutral to alkaline solutions, and this can be assigned to the absorption of the deprotonated **HBO** (anion, this structure is shown in Scheme 1b) being formed at a high pH solution.[35] Similar UV−vis absorption changes are also observed for **NAP**: the original absorption peaks decline in intensity continuously and give two broad absorption bands at 310 and 365 nm by increasing the solution basicity (Figure 1d), which corresponds to the absorption of the **NAP** anion as well. Furthermore, the pK_a values of **HBO** and **NAP** are determined to be around 8.67 and 7.89,

https://doi.org/10.1021/acsphyschemau.2c00036
ACS Phys. Chem Au 2023, 3, 181−189

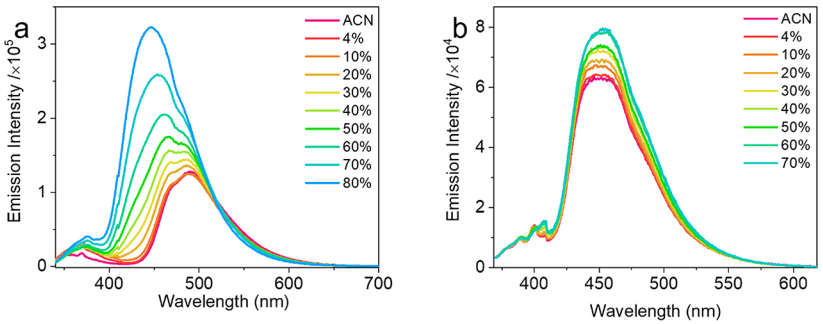

Figure 2. Emission spectra of **HBO** (a) and **NAP** (b) in different fractions of H_2O into ACN solutions with excitation wavelengths of 330 and 356 nm, respectively.

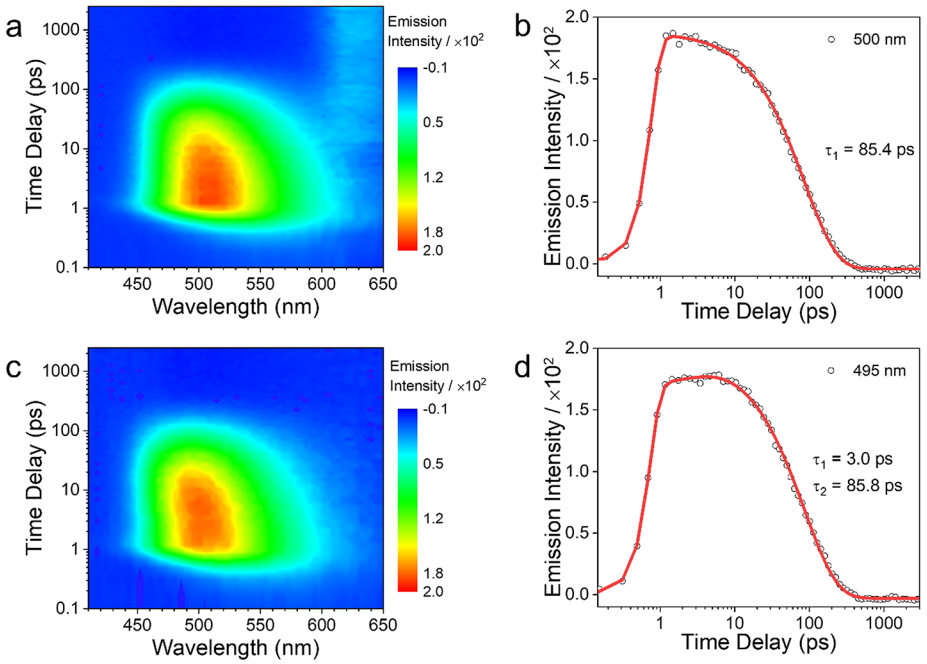

Figure 3. (a,b) Fs-TRF 3D contour of **HBO** in ACN solution upon 267 nm photoexcitation and the kinetics of the characteristic emission band observed at 500 nm. (c,d) Fs-TRF 3D contour of **HBO** in ACN:H_2O (1:1) mixed solution upon 267 nm photoexcitation and the kinetics of the characteristic emission band observed at 495 nm.

respectively,[36] which is also consistent with the fact that the pK_a of naphthol is lower than that of phenol. However, neither the steady-state absorption nor emission spectra are found to vary noticeably by acidification of the solutions to pH 2 for **HBO** (Figure S1a,b). The fluorescence excitation spectra of **HBO** and **NAP** in ACN solution using two excitation wavelengths are depicted in Figure S1d,e.

The emission spectra of **HBO** and **NAP** change when increasing the percentage of water in the ACN/H_2O mixed solutions. As displayed in Figure 2, dual emission is observed for both **HBO** (360 and 490 nm) and **NAP** (400 and 450 nm) in pure ACN solution with the *anti*-enol* emission observed at a shorter wavelength and the *syn*-keto* fluorescence observed at a larger Stokes shift. The emission band at 360 nm redshifts with little increase in intensity for **HBO** by increasing the amounts of water, which can be assigned to the approximately equal contributions from *anti*-enol* and the water-solvated *syn*-enol* species (the structures are shown in Scheme 1b).[33] However, the emission band at 490 nm grows dramatically and blueshifts to 445 nm with a shoulder band at 485 nm. To identify these new emission bands, the emission spectrum of **HBO** in an alkaline environment (pH 10.45) was obtained (Figure S1c). At pH 10.45 solution, **HBO** is completely deprotonated, and the emission peak at 445 nm corresponds to the emission of the singlet excited state of the anion (anion*). Coincidently, this emission band is close to the emission band of **HBO** seen in high-water-content solutions, so both of them can be assigned to the fluorescence of the anion*. The shoulder peak at 485 nm of **HBO** corresponds to the solvent effect on the *syn*-keto* emission.[33] However, the emission spectra of **NAP** do not change much with the variation of H_2O: the flat-shape *syn*-keto* emission band centered at 450 nm becomes sharper and redshifts to 454 nm together with an increased intensity on the shoulder band at 482 nm. Moreover, the deprotonated **NAP** shows similar emission with fluorescence bands at 460 and 482 nm in the pH 10.45 solution (Figure S1c). The emission peaks at 454 and 482 nm are assigned to *syn*-keto* and the anion* species emissions of **NAP** in high-water-content solutions, respectively. However, both the absorption and emission changes observed are limited for **NAP**, implying that water is not the core factor in the deprotonation process for **NAP**. These intriguing results in

https://doi.org/10.1021/acsphyschemau.2c00036
ACS Phys. Chem Au 2023, 3, 181−189

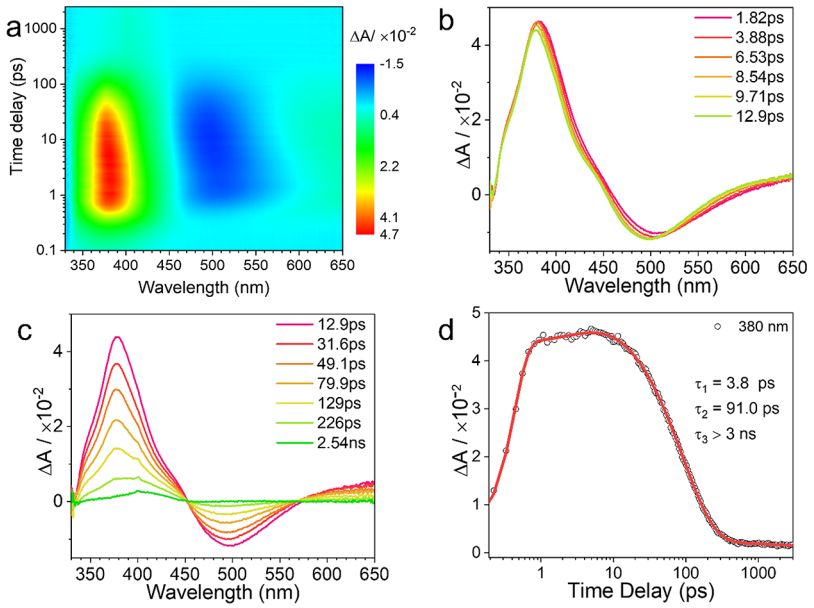

Figure 4. Fs-TA spectra of **HBO** in ACN:H_2O (1:1) solution upon 267 nm photoexcitation, (a) 3D contour plots of the time-resolved absorption spectroscopic responses; (b,c) spectra obtained at different time delays; (d) kinetics of the characteristic absorption band at 380 nm.

aqueous solutions drive us to investigate the origin of the anion* that has not been directly detected and discussed in earlier literature reports. In this case, fs-TRF and fs-TA measurements can be useful to explore the proton transfer mechanisms and the role of water in these reactions.

fs-TRF and fs-TA Experimental Results

fs-TRF measurements realized on a time-resolved upconversion apparatus have been used to predict the radiative decay process of the intermediate after excitation. As shown in Figure 3a,b, a prompt emission band at 500 nm is produced initially and gradually decreases with a time constant of 85.4 ps, which is mainly assigned to the emission of *syn*-keto* and indicates that the ESIPT process takes place within the instrumental response time constant (400 fs). The time constants of the *syn*-keto* closely match with the reported values that are summarized in Table S1. The fs-TRF results of **HBO** in ACN:H_2O (1:1) solution are displayed in Figure 3c,d. The initial emission band obtained at 500 nm also suggests the prompt formation of the *syn*-keto* species within 400 fs. Instead of a decay, the emission band at 500 nm shows an obvious hypochromatic shift to 490 nm and becomes narrower in shape. This could be due to the generation of water-solvated *syn*-keto*, which was reported to give emission at 490 nm.[33] The direct observation of the generation of the water-solvated *syn*-keto* provides the further understanding of the water-surrounded microenvironment. The kinetics at 500 nm could be fitted by two time constants given as 3 and 85.8 ps, which are assigned to the solvation process and the decay of the solvated *syn*-keto*, respectively. Unfortunately, no emission at 450 nm is observed in ACN:H_2O (1:1) solution. Even though the 450 nm emission band obtained in Figure 2 is similar with the anion* of **HBO**, there is still a lack of evidence on how the anion* of **HBO** is generated in the aqueous solution.

Fs-TA was also found to be a powerful technique to detect the intermediates with an ultrashort lifetime and helpful to elucidate the photochemical and photophysical dynamics of molecules.[34,37,38] Therefore, fs-TA experiments were performed for **HBO** in ACN and ACN:H_2O (1:1) solutions to figure out the roles that these solvents played in the ESIPT and subsequent processes. The fs-TA spectra with various delay times and kinetics results for **HBO** in ACN with 267 nm photoexcitation are depicted in Figure S2a,b. According to the previous fs-TRF results, the *syn*-keto* is first populated with an excited-state absorption (ESA) seen at 380 nm together with a stimulated emission (SE) feature at 500 nm (Figure S2a,b). Hereafter, the ESA band at 380 nm and the SE band at 500 nm depopulate and generate a species with an ESA peak at 440 nm with a much lower absorption intensity at 2.86 ns (Figure S2c). The transient species seen at 2.86 ns is in good agreement with the transient absorption features reported for the ground-state *anti*-keto of **HBO**.[30] Therefore, the spectral changes demonstrated in Figure S2c can be assigned to isomerization processes. However, the triplet excited-state species of **HBO** with the transient absorption at 400 and 500 nm is not observed in the present experiment.[30] Kinetics fittings are employed to estimate the lifetimes of the different processes on the characteristic ESA band at 380 nm. Two time constants are eventually obtained as shown in Figure S2d, and they are 99.7 ps and >3 ns. Thus, the ultrafast photophysical dynamics of **HBO** in ACN are elucidated to be as follows: *syn*-keto* is produced from *syn*-enol* via ESIPT within the instrumental response time (400 fs), and the obtained *syn*-keto* generates the *anti*-keto species through isomerization with a time constant of 99.7 ps, which is very consistent with the previous fs-TRF results. Finally, the decay of the *anti*-keto (>3 ns) is out of the range of the temporal delay line of our fs-TA experiments. Similar results are also achieved in hexane as displayed in Figure S3, and these results show that the isomerization process takes a much longer time (283.3 ps) than that in ACN.

To untangle the role of water in the excited-state dynamics of **HBO**, the fs-TA experiments were also performed in ACN:H_2O (1:1) mixed solutions. As depicted in Figure 4, a strong ESA peak at 380 nm shows up with an SE band at 500 nm, and they blueshift to 375 and 490 nm continuously from 1.82 to 12.9 ps, respectively. As discussed above, this process can be assigned to a solvation process (τ = 3.8 ps) from *syn*-

https://doi.org/10.1021/acsphyschemau.2c00036
ACS Phys. Chem Au 2023, 3, 181−189

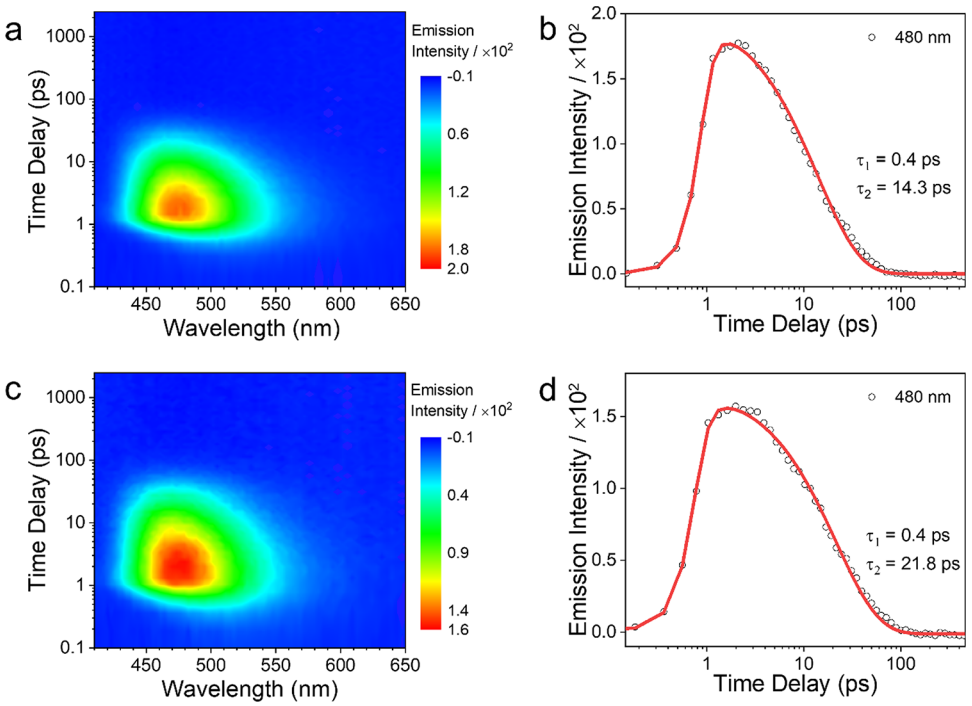

Figure 5. (a,b) Fs-TRF 3D contour of **NAP** in ACN solution upon 267 nm photoexcitation and the kinetics of the characteristic emission band observed at 480 nm. (c,d) Fs-TRF 3D contour of **NAP** in ACN:H_2O (1:1) mixed solution upon 267 nm photoexcitation and the kinetics of the characteristic emission band observed at 480 nm.

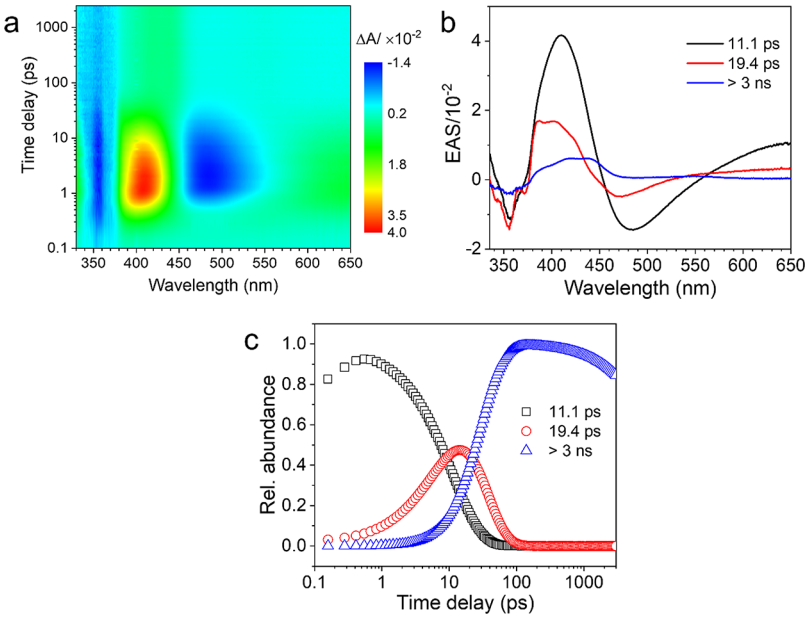

Figure 6. Fs-TA spectra of **NAP** in ACN solution upon 267 nm photoexcitation, (a) 3D contour plots of the time-resolved absorption spectroscopic responses, (b) EAS according to the sequential kinetic models, and (c) time evolution of the state population obtained from the global fitting analysis.

keto* to the water-solvated *syn*-keto* system. Not only the SE band displays the obvious solvated process, but the ESA band also shows this apparent solvation process. Therefore, with the assistance of H_2O in the aqueous solution, the new transient species (water-solvated *syn*-keto*), whose proton donors and acceptors are bridged with H_2O, is obtained after ESIPT as well by direct observation in our study (both in the fs-TA and fs-TRF results). Afterward, the isomerization processes observed in ACN are inhibited significantly, and no ground-state *anti*-keto species is observed. Hence, it is reasonable to draw the conclusion that the photodynamics mechanisms of **HBO** highly depend on the solvents, especially in the presence of water for its hydrogen bonding ability that influences the proton-donating and proton-accepting groups.

NAP is more aromatic than **HBO** and possesses a lower pK_a in the ground state, which indicates that the proton in the hydroxyl group of **NAP** is able to be dissociated more easily than **HBO**. Therefore, further investigations about the

https://doi.org/10.1021/acsphyschemau.2c00036
ACS Phys. Chem Au 2023, 3, 181−189

influence of the proton on the excited-state properties were done by elucidating the excited-state dynamics of **NAP** in ACN and ACN:H_2O (1:1) solutions as well. A point of interest is that unlike the obvious differences obtained for **HBO** in different solutions, the TRF spectra of **NAP** in ACN and ACN:H_2O (1:1) solutions look similar with faster decay rates than those for **HBO** (Figure 5a–d). Taking **NAP** in ACN solution as an example, the characteristic emission bands located at around 480 nm are assigned to the singlet excited state of the **NAP** anion species (anion*) by deprotonation in the singlet excited states as mentioned above, which is mainly due to the much lower pK_a of the singlet excited states of **NAP** in polar solutions (Figure 5a). By fitting the kinetics at 480 nm with a biexponential function, 0.4 and 14.3 ps are achieved, and they correspond to the deprotonation process and the decay process of the anion*, respectively (Figure 5b). In ACN:H_2O (1:1) solution, the lifetime of the anion* is longer than that observed in pure ACN solution (Figure 5d). It is obvious that the ESIPT is inhibited for **NAP**, while the deprotonation takes place first in the singlet excited state. Moreover, the emission of the keto* is too weak to be detected in our fs-TRF spectroscopy, but addition results about this species are discussed in the fs-TA section.

The fs-TA spectra of **NAP** in ACN solution after excitation by 267 nm were acquired. The 3D contour plots and global fitting results utilizing the sequential kinetics scheme[39] from the fs-TA spectra in pure ACN are displayed in Figure 6a–c. As seen in Figure 6b,c, three evolution-associated difference spectra (EAS) are isolated through the global analysis with the lifetimes at 11.1 ps (black), 19.4 ps (red), and >3 ns (blue). The initial ESA species showing absorption bands at 410 and 650 nm with an SE band at 480 nm with a lifetime of 11.1 ps. According to the previous discussion, this initial species can be assigned to the **NAP** anion*, and similar spectra are also observed with the presence of H_2O (as shown in Figure S4). By analogy with the first EAS species, the second EAS species displays hypochromatically shifted bands at 380 nm with a lifetime of 19.4 ps, which indicates a transformation from one species to another and could correspond to the generation of the *syn*-keto* by ESPT. The third EAS species with a broad absorption band at 430 nm is attributed to the absorption of the ground-state *anti*-keto (400 to 450 nm),[10] whose lifetime is >3 ns. Consequently, the dynamics mechanism of **NAP** in ACN solution after 267 nm irradiation is finally elucidated as follows: the excited-state **NAP** is easily deprotonated to generate its anion* followed by ESPT with a time constant of 11.7 ps to produce the *syn*-keto* species, which transforms to the *anti*-keto via isomerization within 19.4 ps.

There is no anion* species that can be observed for **HBO** either in pure ACN solution or aqueous solutions. However, deprotonation takes place first in ACN solution for **NAP**, so this intriguing photochemical pathway drives us to explore the photodynamics of **NAP** in ACN:H_2O (1:1) mixed solution and examine whether water still plays a crucial role in the deprotonation process. The fs-TA spectra and kinetics study of **NAP** in ACN:H_2O (1:1) mixed solution are presented in Figure S4. Surprisingly, the transient absorption patterns of **NAP** in ACN:H_2O (1:1) mixed solution are similar to the spectra obtained in ACN solution. The ESPT and isomerization processes are similar with the results obtained in ACN solution, which are about 8.1 and 26.1 ps, respectively, in the ACN:H_2O (1:1) mixed solution. Thus, it can be concluded that water has little effect on altering the reaction pathways of the excited-state dynamics of **NAP**. These results also help to explain the little difference observed in the fluorescence spectra obtained in different concentrations of H_2O as discussed in a preceding section. Furthermore, by comparing the relative intensities of the third EAS species at ∼410 nm of **NAP** in pure ACN and ACN:H_2O (1:1) mixed solutions, the ground-state *anti*-keto absorption peak is much weaker in the ACN:H_2O (1:1) mixed solution, which implies that the isomerization process is less effective in a protic solution. Figure S5 shows the fs-TA spectra of **NAP** in hexane solution, and these results demonstrate that the *syn*-keto* fluorescence is very weak, and the deprotonation process is not noticeable in hexane. The deuterium isotope effect has been studied both for **HBO** and **NAP**. The fs-TA results in ACN:D_2O (1:1) mixed solutions for **HBO** and **NAP** are displayed in Figures S6 and S7, respectively. Comparing Figure S6 to Figure 4, the photodynamics processes of **HBO** are barely affected by replacing H_2O with D_2O. However, for **NAP**, when H_2O is replaced by D_2O, the ESPT process is slightly extended from 8.1 (Figure S4) to 11.1 ps (Figure S7) due to the deuterium isotope effect. The different behaviors observed between **HBO** and **NAP** after irradiation could be due to the structural differences, especially with the introduction of naphthalene in **NAP**.

CONCLUSIONS

The photophysical and photochemical mechanisms of **HBO** and **NAP** and the influence of solvent effects have been investigated by steady-state absorption, steady-state emission, and fs-TRF and fs-TA techniques in different solutions. As demonstrated in Scheme 2, the detailed mechanisms of **HBO** and **NAP** under 267 nm photoexcitation reveal that the photodynamics mechanisms of **HBO** and **NAP** are different and that ESIPT is not observed for **NAP**. In ACN solutions, **HBO** generates the *syn*-keto* tautomer first, and this is followed by the isomerization process. However, in ACN:H_2O (1:1) mixed solutions, the proton-donating and proton-accepting groups are bridged with H_2O, and the water-solvated *syn*-keto* is formed immediately after ESIPT, and no isomerization is observed in the following photodynamics processes in aqueous solution. Very surprisingly, the anion* species is able to be observed in both solvents used here in the

Scheme 2. Photodynamics of HBO (Top) and NAP (Bottom) under 267 Photoexcitation[a]

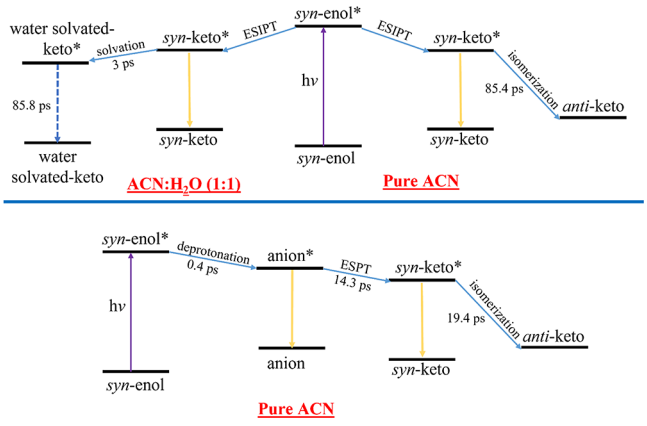

[a]The time constants representing different processes obtained from fs-TRF are primarily considered to be listed on the scheme.

https://doi.org/10.1021/acsphyschemau.2c00036
ACS Phys. Chem Au 2023, 3, 181–189

experiments for **NAP** within a sub-picosecond timescale. Thus, we propose that **NAP** goes through an ESPT process instead of an ESIPT pathway, in which the *syn*-keto* is generated from the anion*. The facile excited-state deprotonation observed in ACN for **NAP** instead of **HBO** may be associated with the lower pK_a of **NAP** with an expanded aromatic ring from benzene to naphthalene.

■ ASSOCIATED CONTENT

Supporting Information

The Supporting Information is available free of charge at https://pubs.acs.org/doi/10.1021/acsphyschemau.2c00036.

Four-level photocycle of the ESIPT process; energy diagram and detailed information of **HBO** and **NAP** after photoexcitation based on the literature; steady-state absorption and emission spectra of **HBO** in acidic solutions; anion* emission of **HBO** and **NAP**; fs-TA spectra of **HBO** in ACN, hexane, and ACN:D_2O (1:1)solution and **NAP** in ACN:H_2O (1:1), hexane, and ACN:D_2O (1:1) solutions with 267 excitations (PDF)

■ AUTHOR INFORMATION

Corresponding Authors

Lili Du − *School of Life Sciences, Jiangsu University, Zhenjiang 212013, P.R. China; Department of Chemistry, The University of Hong Kong, Hong Kong 999077, P.R. China;* orcid.org/0000-0002-9712-3925; Email: dulili@ujs.edu.cn

David Lee Phillips − *Department of Chemistry, The University of Hong Kong, Hong Kong 999077, P.R. China; Guangdong-Hong Kong-Macao Joint Laboratory of Optoelectronic and Magnetic Functional Materials, Hong Kong 999077, P.R. China;* orcid.org/0000-0002-8606-8780; Email: phillips@hku.hk

Authors

Runhui Liang − *School of Life Sciences, Jiangsu University, Zhenjiang 212013, P.R. China; Department of Chemistry, The University of Hong Kong, Hong Kong 999077, P.R. China*

Yuanchun Li − *Department of Chemistry, The University of Hong Kong, Hong Kong 999077, P.R. China*

Zhiping Yan − *Institute of Advanced Materials (IAM), Nanjing Tech University (Nanjing Tech), Nanjing 211816, P.R. China*

Xueqin Bai − *Department of Chemistry, The University of Hong Kong, Hong Kong 999077, P.R. China*

Wenquan Lai − *Department of Chemistry, The University of Hong Kong, Hong Kong 999077, P.R. China*

Complete contact information is available at: https://pubs.acs.org/10.1021/acsphyschemau.2c00036

Author Contributions

CRediT: **Runhui Liang** data curation (equal), formal analysis (equal), investigation (equal), methodology (equal), writing-original draft (equal); **Yuanchun Li** data curation (equal), formal analysis (supporting), investigation (equal), methodology (supporting); **Zhiping Yan** data curation (supporting), formal analysis (supporting), investigation (supporting), methodology (supporting); **Xueqin Bai** data curation (supporting), formal analysis (supporting), investigation (supporting), methodology (supporting); **Wenquan Lai** formal analysis (supporting), investigation (supporting), methodology (supporting); **Lili Du** conceptualization (equal), data curation (equal), formal analysis (supporting), investigation (equal), methodology (equal), supervision (equal), writing-original draft (equal), writing-review & editing (equal); **David Lee Phillips** conceptualization (equal), formal analysis (supporting), funding acquisition (lead), investigation (supporting), project administration (equal), resources (lead), supervision (lead), writing-review & editing (equal).

Notes

The authors declare no competing financial interest.

■ ACKNOWLEDGMENTS

This work was supported by grants from the Hong Kong Research Grants Council (GRF 17302419; GRF 17316922), The University of Hong Kong Development Fund 2013−2014 project "New Ultrafast Spectroscopy Experiments for Shared Facilities", the Major Program of Guangdong Basic and Applied Research (2019B030302009), the Guangdong-Hong Kong-Macao Joint Laboratory of Optoelectronic and Magnetic Functional Materials (2019B121205002), and the Key-Area Research and Development Program of Guangdong Province (2020B0101370003).

■ REFERENCES

(1) Weller, A. Über die Fluoreszenz der Salizylsäure und verwandter Verbindungen. *Naturwissenschaften* **1955**, *42*, 175−176.

(2) Sedgwick, A. C.; Wu, L.; Han, H. H.; Bull, S. D.; He, X. P.; James, T. D.; Sessler, J. L.; Tang, B. Z.; Tian, H.; Yoon, J. Excited-state intramolecular proton-transfer (ESIPT) based fluorescence sensors and imaging agents. *Chem. Soc. Rev.* **2018**, *47*, 8842−8880.

(3) Padalkar, V. S.; Seki, S. Excited-state intramolecular proton-transfer (ESIPT)-inspired solid state emitters. *Chem. Soc. Rev.* **2016**, *45*, 169−202.

(4) Sheng, H.; Hu, Y.; Zhou, Y.; Fan, S.; Cao, Y.; Zhao, X.; Yang, W. A highly selective ESIPT-based fluorescent probe with a large Stokes shift for the turn-on detection of cysteine and its application in living cells. *Dyes Pigm.* **2019**, *160*, 48−57.

(5) Kwon, J. E.; Park, S. Y. Advanced organic optoelectronic materials: harnessing excited-state intramolecular proton transfer (ESIPT) process. *Adv. Mater.* **2011**, *23*, 3615−3642.

(6) Massue, J.; Felouat, A.; Vérité, P. M.; Jacquemin, D.; Cyprych, K.; Durko, M.; Sznitko, L.; Mysliwiec, J.; Ulrich, G. An extended excited-state intramolecular proton transfer (ESIPT) emitter for random lasing applications. *Phys. Chem. Chem. Phys.* **2018**, *20*, 19958−19963.

(7) Lampkin, B. J.; Nguyen, Y. H.; Karadakov, P. B.; VanVeller, B. Demonstration of Baird's rule complementarity in the singlet state with implications for excited-state intramolecular proton transfer. *Phys. Chem. Chem. Phys.* **2019**, *21*, 11608−11614.

(8) Kanda, T.; Momotake, A.; Shinohara, Y.; Sato, T.; Nishimura, Y.; Arai, T. Photoinduced Proton Transfer in 2-(2′-Hydroxynaphthalenyl)benzoxazole: Observation of Fluorescence with a Small Stokes Shift Induced by Excited-State Intramolecular Proton Transfer. *Bull. Chem. Soc. Jpn.* **2009**, *82*, 118−120.

(9) Azarias, C.; Budzák, Š.; Laurent, A. D.; Ulrich, G.; Jacquemin, D. Tuning ESIPT fluorophores into dual emitters. *Chem. Sci.* **2016**, *7*, 3763−3774.

(10) Iijima, T.; Momotake, A.; Shinohara, Y.; Sato, T.; Nishimura, Y.; Arai, T. Excited-state intramolecular proton transfer of naphthalene-fused 2-(2′-hydroxyaryl)benzazole family. *J. Phys. Chem. A* **2010**, *114*, 1603−1609.

(11) Ignasiak, M. T.; Houée-Levin, C.; Kciuk, G.; Marciniak, B.; Pedzinski, T. A reevaluation of the photolytic properties of 2-

hydroxybenzophenone-based UV sunscreens: are chemical sunscreens inoffensive? *ChemPhysChem* **2015**, *16*, 628−633.
(12) Liu, B.; Wang, J.; Zhang, G.; Bai, R.; Pang, Y. Flavone-based ESIPT ratiometric chemodosimeter for detection of cysteine in living cells. *ACS Appl. Mater. Interfaces* **2014**, *6*, 4402−4407.
(13) Dai, J.; Han, J.; Chen, X.; Fang, W.; Ma, J.; Phillips, D. L. Water-assisted self-photoredox of 2-(1-hydroxyethyl)-9,10-anthraquinone through a triplet excited state intra-molecular proton transfer pathway. *Phys. Chem. Chem. Phys.* **2015**, *17*, 27001−27010.
(14) Schmidtke, S. J.; Underwood, D. F.; Blank, D. A. Following the solvent directly during ultrafast excited state proton transfer. *J. Am. Chem. Soc.* **2004**, *126*, 8620−8621.
(15) Chung, M. W.; Lin, T. Y.; Hsieh, C. C.; Tang, K. C.; Fu, H.; Chou, P. T.; Yang, S. H.; Chi, Y. Excited-state intramolecular proton transfer (ESIPT) fine tuned by quinoline-pyrazole isomerism: pi-conjugation effect on ESIPT. *J. Phys. Chem. A* **2010**, *114*, 7886−7891.
(16) Yin, H. Q.; Yin, F.; Yin, X. B. Strong dual emission in covalent organic frameworks induced by ESIPT. *Chem. Sci.* **2019**, *10*, 11103−11109.
(17) Gao, M.; Hu, Q.; Feng, G.; Tang, B. Z.; Liu, B. A fluorescent light-up probe with "AIE + ESIPT" characteristics for specific detection of lysosomal esterase. *J. Mater. Chem. B* **2014**, *2*, 3438−3442.
(18) Chen, L.; Wu, D.; Lim, C. S.; Kim, D.; Nam, S. J.; Lee, W.; Kim, G.; Kim, H. M.; Yoon, J. A two-photon fluorescent probe for specific detection of hydrogen sulfide based on a familiar ESIPT fluorophore bearing AIE characteristics. *Chem. Commun.* **2017**, *53*, 4791−4794.
(19) Goodman, J.; Brus, L. E. Proton transfer and tautomerism in an excited state of methyl salicylate. *J. Am. Chem. Soc.* **2002**, *100*, 7472−7474.
(20) Ciuciu, A. I.; Skonieczny, K.; Koszelewski, D.; Gryko, D. T.; Flamigni, L. Dynamics of Intramolecular Excited State Proton Transfer in Emission Tunable, Highly Luminescent Imidazole Derivatives. *J. Phys. Chem. C* **2013**, *117*, 791−803.
(21) Lochbrunner, S.; Stock, K.; Riedle, E. Direct observation of the nuclear motion during ultrafast intramolecular proton transfer. *J. Mol. Struct.* **2004**, *700*, 13−18.
(22) Lochbrunner, S.; Wurzer, A. J.; Riedle, E. Ultrafast excited-state proton transfer and subsequent coherent skeletal motion of 2-(2′-hydroxyphenyl)benzothiazole. *J. Chem. Phys.* **2000**, *112*, 10699−10702.
(23) Tsutsui, Y.; Zhang, W.; Ghosh, S.; Sakurai, T.; Yoshida, H.; Ozaki, M.; Akutagawa, T.; Seki, S. Electrically Switchable Amplified Spontaneous Emission from Liquid Crystalline Phase of an AIEE-Active ESIPT Molecule. *Adv. Opt. Mater.* **2020**, *8*, No. 1902158.
(24) Chevalier, K.; Wolf, M. M.; Funk, A.; Andres, M.; Gerhards, M.; Diller, R. Transient IR spectroscopy and ab initio calculations on ESIPT in 3-hydroxyflavone solvated in acetonitrile. *Phys. Chem. Chem. Phys.* **2012**, *14*, 15007−15020.
(25) Bader, A. N.; Ariese, F.; Gooijer, C. Proton Transfer in 3-Hydroxyflavone Studied by High-Resolution 10 K Laser-Excited Shpol'skii Spectroscopy. *J. Phys. Chem. A* **2002**, *106*, 2844−2849.
(26) McMorrow, D.; Kasha, M. Proton-transfer spectroscopy of 3-hydroxyflavone in an isolated-site crystal matrix. *Proc. Natl. Acad. Sci. U. S. A.* **1984**, *81*, 3375−3378.
(27) Abou-Zied, O. K.; Jimenez, R.; Thompson, E. H. Z.; Millar, D. P.; Romesberg, F. E. Solvent-Dependent Photoinduced Tautomerization of 2-(2′-Hydroxyphenyl)benzoxazole. *J. Phys. Chem. A* **2002**, *106*, 3665−3672.
(28) Roohi, H.; Hejazi, F.; Mohtamedifar, N.; Jahantab, M. Excited state intramolecular proton transfer (ESIPT) in 2-(2′-hydroxyphenyl)benzoxazole and its naphthalene-fused analogs: a TD-DFT quantum chemical study. *Spectrochim. Acta, Part A* **2014**, *118*, 228−238.
(29) Arthen-Engeland, T.; Bultmann, T.; Ernsting, N. P.; Rodriguez, M. A.; Thiel, W. Singlet excited-state intramolecular proton tranfer in 2-(2t'-hydroxyphenyl) benzoxazole: spectroscopy at low temperatures, femtosecond transient absorption, and MNDO calculations. *Chem. Phys.* **1992**, *163*, 43−53.
(30) Stephan, J. S.; Grellmann, K. H. Photoisomerization of 2-(2'-Hydroxyphenyl)benzoxazole. Formation and Decay of the Trans-Keto Tautomer in Dry and in Water-Containing 3-Methylpentane. *J. Phys. Chem.* **1995**, *99*, 10066−10068.
(31) Wang, H.; Zhang, H.; Abou-Zied, O. K.; Yu, C.; Romesberg, F. E.; Glasbeek, M. Femtosecond fluorescence upconversion studies of excited-state proton-transfer dynamics in 2-(2′-hydroxyphenyl)-benzoxazole (HBO) in liquid solution and DNA. *Chem. Phys. Lett.* **2003**, *367*, 599−608.
(32) Das, K.; Sarkar, N.; Ghosh, A. K.; Majumdar, D.; Nath, D. N.; Bhattacharyya, K. Excited-State Intramolecular Proton Transfer in 2-(2-Hydroxyphenyl)benzimidazole and -benzoxazole: Effect of Rotamerism and Hydrogen Bonding. *J. Phys. Chem.* **1994**, *98*, 9126−9132.
(33) Abou-Zied, O. K. The role of water in solvating the hydrogen-bonding center of 2-(2′-hydroxyphenyl)benzoxazole. *Chem. Phys.* **2007**, *337*, 1−10.
(34) Liang, R.; Xiong, W.; Bai, X.; Du, L.; Phillips, D. L. Direct Observation of the Triplet Excited States and Dynamics of Platinum(II)-Tetraphenylethylene Complexes by Time-Resolved Transient Absorption Spectroscopy. *J. Phys. Chem. C* **2021**, *125*, 11432−11439.
(35) Krishnamurthy, M.; Dogra, S. K. Proton transfer of 2-(2′-hydroxyphenyl)benzoxazole in the excited singlet state. *J. Photochem.* **1986**, *32*, 235−242.
(36) Novo, M.; Mosquera, M.; Prieto, F. R. Prototropic equilibria of 2-pyridylbenzimidazoles in aqueous solution. *Can. J. Chem.* **1992**, *70*, 823−827.
(37) Du, L.; Qiu, Y.; Lan, X.; Zhu, R.; Phillips, D. L.; Li, M. D.; Dutton, A. S.; Winter, A. H. Direct Detection of the Open-Shell Singlet Phenyloxenium Ion: An Atom-Centered Diradical Reacts as an Electrophile. *J. Am. Chem. Soc.* **2017**, *139*, 15054−15059.
(38) Xiong, W.; Du, L.; Lo, K. C.; Shi, H.; Takaya, T.; Iwata, K.; Chan, W. K.; Phillips, D. L. Control of Electron Flow Direction in Photoexcited Cycloplatinated Complex Containing Conjugated Polymer-Single-Walled Carbon Nanotube Hybrids. *J. Phys. Chem. Lett.* **2018**, *9*, 3819−3824.
(39) van Stokkum, I. H. M.; Larsen, D. S.; van Grondelle, R. Global and target analysis of time-resolved spectra. *Biochim. Biophys. Acta, Bioenerg.* **2004**, *1657*, 82−104.

https://doi.org/10.1021/acsphyschemau.2c00036
ACS Phys. Chem Au 2023, 3, 181−189